

# Comparison of Early Age Resistivity Development Between Ordinary Portland Cement and Calcium Sulfoaluminate Cement

J. Zhang<sup>\*</sup>, Z. Li

*The Hong Kong University of Science and Technology, Clear Water Bay,  
Kowloon, Hong Kong, China*

## Abstract

In this study, the early age resistivity development has been measured for ordinary Portland cements (OPC) and calcium sulfoaluminate cements (CSA) using a non-contacting electrical resistivity measurement. It is found that the hydration process of OPC can be characterized by the resistivity curves. Different hydration stages can be distinguished from the rate of resistivity curves compared with the temperature development. However, the resistivity development of the CSA paste is quite different from that of OPC paste. The CSA cement pastes had higher resistivity values than OPC with the same water to cement ratio, and showed an uncommon delta-shaped resistivity phenomenon. The mechanism of these behaviors has been investigated to explore the relationship between the resistivity and the hydration developments.

*Keywords:* Electrical resistivity; Hydration; Early age; Ordinary Portland cement; Calcium sulfoaluminate cement

## 1. Introduction

One of the most promising methods used to investigate the complex hydration process of cement-based materials is the electrical technique, which is based on monitoring the electrical properties during the initial setting and in the subsequent hardening period [1]. The electrical method has advantages over other methods in terms of sensitivity and fast processing. Because the electrical parameters reflect the change of nature, mobility, concentration and distribution of the charge carriers, they are sensitive to the complex factors affecting the hydration and microstructure of cement-based media, such as different water/cement (W/C) ratios, the different chemical composition of cement and its hydration products, and other factors which can alter the nature of the hydration process. Recent developments of experimental techniques and computational support allow fast processing, and accurate and continuous

---

<sup>\*</sup> Corresponding author. Tel.: 852-64056569; fax: 852-23581534.  
E-mail address: [zhangjie@ust.hk](mailto:zhangjie@ust.hk) (Zhang Jie)

data acquisition, as the non-contacting electrical resistivity measurement device used in this study. The electrical resistivity-time plots are thus very informative and can be regarded as the fingerprints of cement hydration. The newly non-contacting electrical resistivity apparatus (Fig.1) used in the present work is a patent of Li and Li (United States Patent 6639401) [2]. Studies done by this instrument [3, 4] shows that this new contactless resistivity measurement device can provide a non-destructive and objective way to determine and assess both the setting time and some mechanical properties of the cement during the entire setting process, and can provide a sensitive and effective way to characterize the hydration of cement-based materials.

This present study investigates the composition of the cement variable on the resistivity of the hardened pastes. Because the understanding of the nature and early age behavior of cement paste is of prime important in making qualified concrete products because cement is the most active component of mortar and concrete [5]. Two types of cement (OPC and CSA) with quite different compositions are studied under the variable W/C ratios. All tests reported here were made in the state of setting and hardening and measured at relatively low A.C. frequencies (1 KHz), which means that the changes in electrical resistivity can be attributed to changes in the number and /or the mobility of charge carrying ions.

## 2. Raw materials and sample preparation

The OPC used was Hong Kong manufactured ordinary Portland cement meeting the requirement of ASTM Type I.

CSA cement used here was commercial Chinese rapid hardening calcium sulfoaluminate cement from the Chinese Building Materials Academy. CSA cement has initially been developed in China in the 1970's [6]. The annual production has now reached more than million tons. It is a promising high-performance material due to its rapid strength gain and better durability in a range of aggressive environments [7]. Because of its low energy requirement for production, CSA cement is also regarded as a green cement, providing environmental benefit, notably the reduced emission of carbon dioxide as compared with Portland cement production [8]. Similar to Portland cement, CSA cement is made commercially by inter grinding clinker to a fine powder together with added gypsum to get the acceptable setting times and suitable strength development [9]. However, it is substantially different from OPC in chemical composition. The most distinctive feature of CSA cements is their content of yeelite or tetracalcium trialuminate sulfate  $C_4A_3\bar{S}$  (cement chemistry abbreviations: C=CaO, S=SiO<sub>2</sub>, A=Al<sub>2</sub>O<sub>3</sub>, F=Fe<sub>2</sub>O<sub>3</sub>,  $\bar{S}$ =SO<sub>3</sub>, H=H<sub>2</sub>O) and belite (C<sub>2</sub>S). It also contains other phases like C<sub>4</sub>AF, C<sub>12</sub>A<sub>7</sub>, C<sub>3</sub>A and

$C_6AF_2$ . Ettringite ( $C_6A\bar{S}_3H_{32}$ ) and monosulfate ( $C_4A\bar{S}H_{12}$ ) are the main crystal products of CSA cement.  $Al_2O_3$  and  $Fe_2O_3$  are the main gel products. Some C-S-H phases are also produced [10].

Table (1) shows the chemical compositions of OPC and CSA tested from the XRF method. Portland cements are normally inter-ground with 2-5% calcium sulfate, whereas calcium sulfate is added to CSA clinkers at much higher levels, 38% by weight in this study. These large additions affect the hydration process and mineralogy of the CSA paste fraction [9]. All samples were conducted under an ambient temperature of  $22\pm 2^\circ C$ . The W/C ratios (0.3, 0.38, 0.44 to 0.55) used here were selected from experience: it was sufficient to form workable pastes but not so water rich as to cause problems of bleed and laitance. Notation used to represent the samples in this paper: P03, P038, P044 and P055 represent the OPC cement with W/C=0.3, 0.38, 0.44 and 0.55, respectively; S03, S038, S044, S055 represent the CSA cement with W/C=0.3, 0.38, 0.44 and 0.55, respectively. The pastes were mixed for 2 min in a planetary-type mixer at 45 rpm followed by 2 min at 90 rpm.

**Table 1** Chemical composition of OPC and CSA cement

Cements	SiO <sub>2</sub>	Al <sub>2</sub> O <sub>3</sub>	Fe <sub>2</sub> O <sub>3</sub>	CaO	SO <sub>3</sub>	MgO	Others
OPC	19.45	5.50	4.00	63.51	5.60	0.97	0.97
CSA	4.05	18.71	1.61	50.64	22.59	1.26	1.14

### 3. Electrical resistivity methods and results

#### 3.1 Non-contacting resistivity measurements

The measuring system for electrical resistivity is shown in Fig. (1). This non-contacting resistivity measurement is based on the Faraday's law of induction (more generally, the law of electromagnetic induction). It works like a transformer. The wire-wound coil acts as the primary and the cement-based ring-shaped specimen acts as the secondary of the transformer. When an AC with a 1 kHz frequency sine wave is applied on the primary coil, a toroidal current will be induced in the secondary. The toroidal current is measured by another ring-shaped current transducer surrounding the specimen. Therefore, the resistivity of the specimen can be easily calculated. This apparatus has completely eliminated the electrodes problems commonly occurred in traditional methods, such as polarization, gas releasing and contacting problems. The reliability of this new device has been calibrated using a standard solution and the results indicate the apparatus has high accuracy. Hence, it can accurately record the resistivity developments of cement-based materials. The temperature development of the samples can be also recorded by inserting the thermocouples.

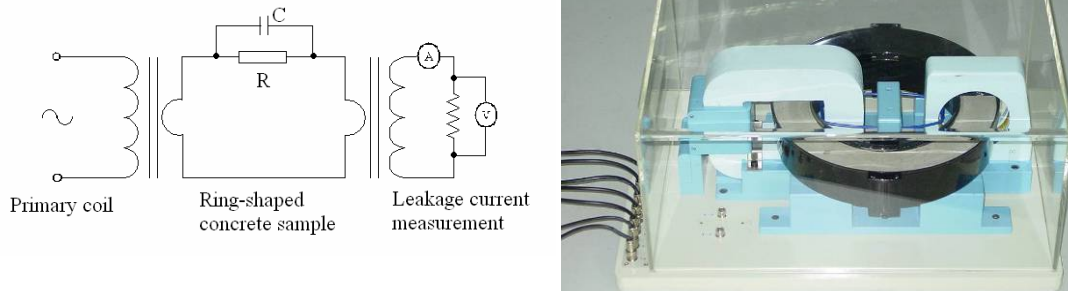


**Fig.1** Equivalent circle and picture of the non-contacting electrical resistivity measurement device

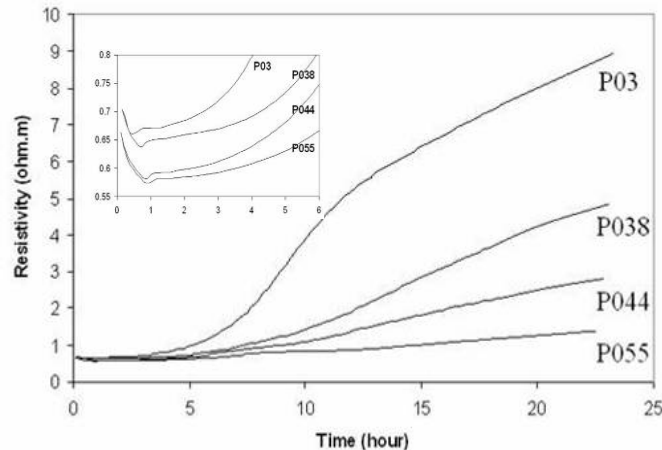
The test procedure is quite easy. Right after mixing, the mixture is cast into the ring-shaped mould that is kept at 100% relative humidity and the initial resistivity values can be recorded soon. The sampling period is 1 min and operation is continuous. All samples are tested without any breakage and hydration cease. The data recording program can be stopped at any time as needed.

### 3.2 OPC resistivity results

Fig. (2) shows the effect of W/C ratio on the electrical resistivity of the neat OPC paste. All the samples have the similar behaviors in the resistivity-time curve. The resistivity begins with a decrease corresponding to the dissolution of ions from cement in water. It is clear that the time to get the minimum resistivity is delayed and reduced with the W/C ratio increase as shown in the inset figure in Fig. (2). The presence of more water in the higher W/C ratios samples can dissolve more ions in the pore solution. Therefore, the increase in the initial W/C ratio of the paste results in an increase in the time at which the minimum resistivity appears and the time at which the slow increase of resistivity transits to the fast increase.

After the resistivity minimum, the increase observed in the resistivity response shows different slopes, which are also observed in the rate of resistivity curve (Fig. 5-a). For P03, during the period from 0.5 to 4 hours of hydration, the resistivity increase is very small (change only from 0.66 to 0.78 ohm.m). After reaching the minimum point, C-H forms in solution, which reduces the ion concentration and allows additional ions from cement particles dissolved. The system enters a competition period which correlates with the very slow development in the resistivity curves. The resistivity of the sample with higher W/C ratio shows longer competition period than the lower one, because higher W/C ratio leads to more free water to dissolve more ions. Hydration products grow at a rate determined by ionic species availability at the reaction sites. So the saturation of the solution is delayed and the hydration process is retarded. This retarding phenomenon agrees with the setting time tested by the Vicat method. And the setting time happened at the end of the II period shown in Table. (2).

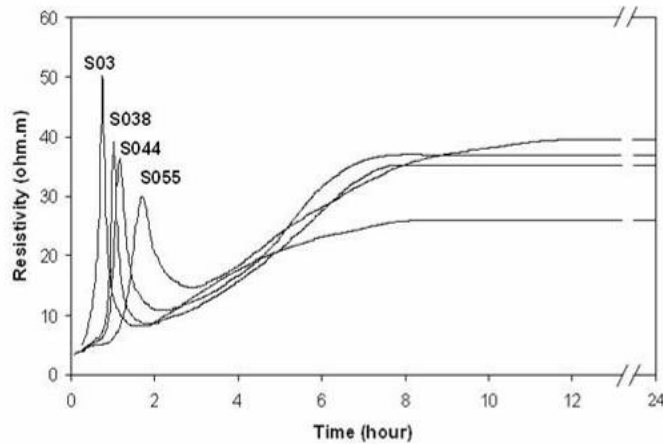
After the setting time, the rate of cement hydration increases sharply due to the breakdown of the hydrate layer, nucleation, and the growth of hydrates. A faster increase is observed in P03 curve from 4 to 9 hours after mixing. At about 9 hours of hydration, the rate of resistivity reaches the maximum. This fast increase is followed by another period of increase between 9 to 15 hours with a small slope. With the hydration degree increases, the resistivity of the sample increases due to the increase of the solid phase and their interconnection, which will block the way of transportation of the ionic conductors in the pore solution. After 15 hours, the increase of resistivity shows a relatively slow and stable rate.



**Fig.2** Resistivity developments of OPC samples during the first 24 hours of hydration

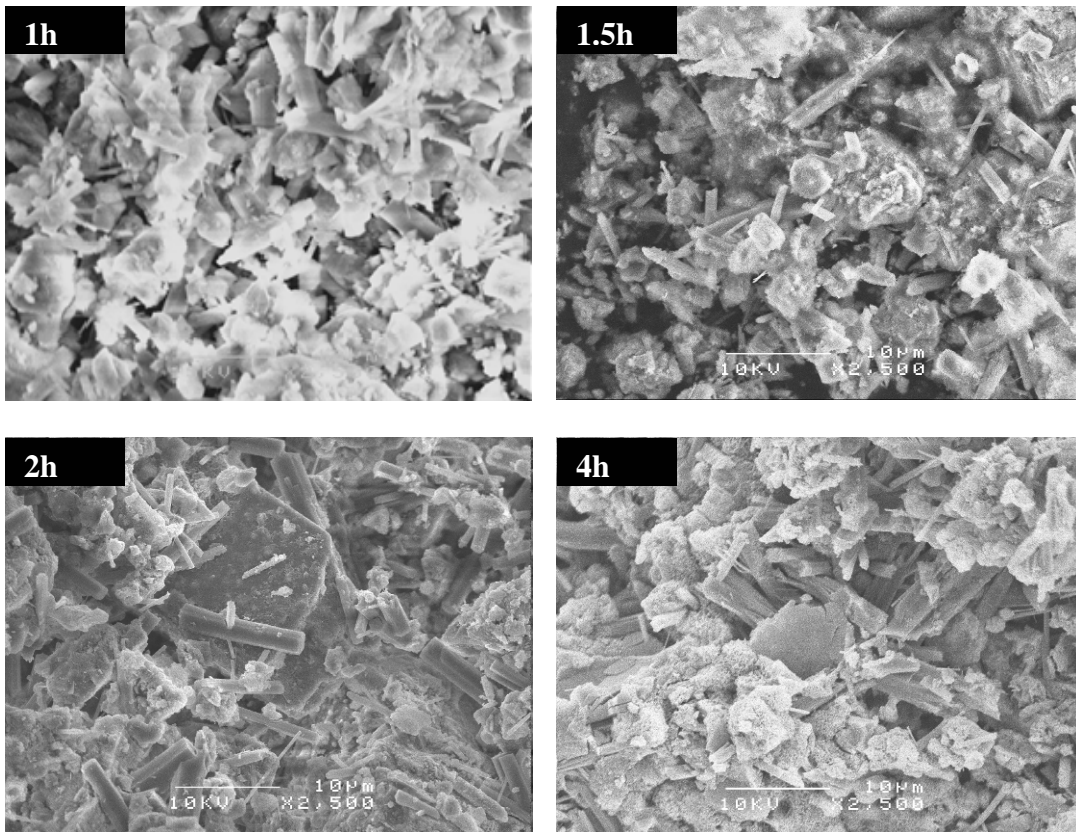
### 3.3 CSA resistivity results

We have observed a phenomenon of a delta-shaped peak in resistivity at the early hydration stage of CSA cement pastes as shown in Fig. (3). This phenomenon was reported and discussed by Li and Zhang [11]. All the CSA samples have this delta phenomenon in resistivity-time curve. After the slow increase, the resistivity of CSA paste increases rapidly to a very high value, larger than 30 ohm.m (Fig.3), at the very early hydration stage. The electrical resistivity of OPC sample with the same W/C at the same time of hydration is less than 1 ohm.m (Fig.2), showing a remarkable difference. And this high resistivity of CSA paste is even larger than its hardened sample. However, it lasts only a few minutes and is followed by a sharp decrease to the level before the sharp increase, showing a typical delta function shape. Then the resistivity comes back to the normal development. Finally, about 10 h after casting, there is no significant change of resistivity showing that the major hydration of CSA cement has finished. With the W/C increased, the setting time is prolonged and the longer time is also needed to reach the resistivity crest. The value of resistivity crest decreases with more water in the mixture.



**Fig.3** Resistivity developments of CSA samples during the first 24 hours of hydration

The electrical resistivity is sensitive to the microstructure changes of cementitious materials. In order to learn the interesting resistivity development of CSA cement, scanning electron microscope (SEM) was employed to observe the microstructure changes at different hydration ages. The six images in Fig. (4) are the SEM pictures of CSA paste with  $w/c=0.55$  hydrated for 1h, 1.5h, 2h, 4h, 7h and 24h at room temperature. From the figure, we can see that with the hydration going on, more and more hydration products are formed. The needle-like and prismatic crystals are ettringite, which is the primary product of CSA cement. At



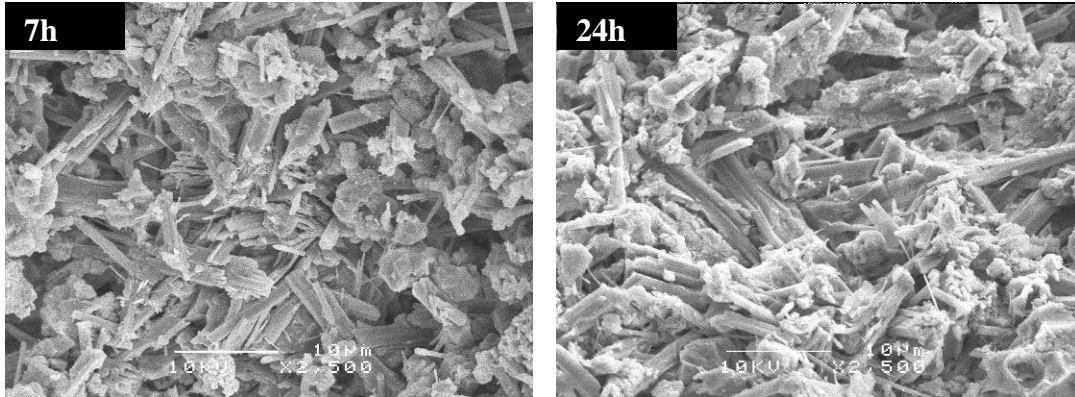


**Fig.4** SEM figures with 2500 magnification of CSA cement with  $w/c=0.55$ . Hydration ages are 1h, 1.5h, 2h, 4h, 7h and 24h, respectively.

about 1.5h, after the final set, the ettringite forms as 3 to 5  $\mu\text{m}$  long. Formation of this initial network corresponds to the loss of physical plasticity. After 2h's hydration, the ettringite becomes more and thicker. These crystals show well prismatic-shape with lengths up to 5~10  $\mu\text{m}$ . They coalesce and join cement particles forming the ettringite network. The other major hydration product is monosulfate, however it is difficult to recognize it from other amorphous unhydrated cement and gel products in the SEM pictures because monosulfate is low crystallinity. In the 7h and 24h's microstructure pictures, more hydration products exist and form the crystal and gel network. It can be observed that the microstructures of 7h's and 24h's are similar to each other, with the similar amount of hydration products and similar density of the structure. This shows the small change of the microstructure after the very early hydration stage, which is corresponding to the small change after 7h in resistivity development. We believe that the microstructure changes during the hydration process are related to the hydration stages in the resistivity-time curves.

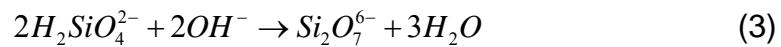
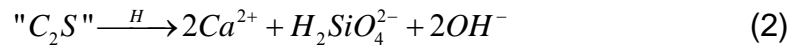
#### 4. Discussions

An attempt has been made in this study to relate the electrical resistivity and its rate curves to the temperature development of hydration for both OPC and CSA paste during the first hours after mixing with water. For OPC paste, all the samples with different W/C ratios have the similar behaviors of the resistivity and the temperature developments. Here we only show the typical resistivity, rate of resistivity and temperature developments of P03 during the first 24 hours of hydration. The progress of the hydration reaction with time involves five stages as shown in Fig. (5-a):

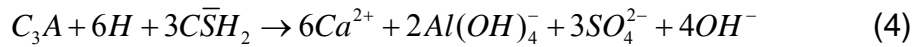
- I—dissolution stage (0-0.5 hour);
- II—competition stage (0.5-4 hour);
- III—acceleration stage (4-9 hour);
- IV—deceleration stage (9-15 hour); and

- V—steady hardening stage (after 15 hour).

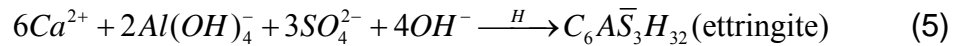
In Stage I, upon mixing cement with water several hydration reactions take place. The decrease of electrical resistivity is due to the increase of ionic concentrations and the mobility of these ions. After the initial solubilization, the formation of the solid hydration products occurs from the solution phase or at a solid-solution interface. The two most important components of Portland cements are tricalcium silicate ( $C_3S$ ) and tricalcium aluminate ( $C_3A$ ) because their hydration reactions are the initial building blocks of the resulting chemical bonded cementitious materials [12]. The hydration of  $C_3S$  has the following reactions involved [13] during the various stages of hydration (No interaction with the other clinker minerals has been assumed in the following hydration reactions.):



The main reactions which  $C_3A$  goes through in the presence of gypsum ( $C\bar{S}H_2$ ) are as follows:



At the end of stage I (about 0.5 hour after mixing) the following product is formed:

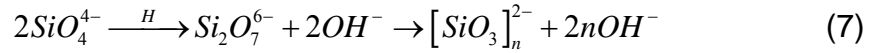


As the water within the pore system becomes saturated with the ions [5], the resistivity reaches the minimum point, showing the end of the first hydration period. Therefore, it may be well concluded that the resistivity development during this stage is mainly due to the presence of the ionic species described in Eq. (1) to (4), and other alkali impurity ions.

In Stage II, the ions are readily absorbed by the formation of a thin layer of hydration products, mainly as ettringite (AFt) and calcium silicate (C-H) hydrates. These hydrates form an envelope around the unhydrated cement grains. These effects reduce the ion concentration and meanwhile allow additional ions from cement particles dissolved. Thus, this competition of consuming and releasing ions leads to a slow development in the resistivity-time curve and a slow increase of the temperature curve as well. Near the end of the competition period, the rate of cement hydration increases sharply because of the breakdown of the hydrate layer, nucleation, and the growth of hydrates, leading to setting. So, point 2, the transition from stage II to stage III, is at the time of setting as shown in the Fig. (5-a).

In Stage III, at the beginning, C-H crystallize from the solution with concomitant development of C-S-H from the surface of  $C_3S$  to form a coating covering grain and the reaction of  $C_3S$  proceeds rapidly. The rapid

increase of resistivity is related to a relatively small but significantly decrease in the number of ionic species. The temperature in the samples increases rapidly to reach the maximum mainly due to the hydration of the tricalcium silicate and the tricalcium aluminate. At the end of stage II or beginning of stage III, the following reactions occur:



In Stage IV, the reaction rate is decelerated. The overall  $C_3S$  and  $C_3A$  reactions are:



In Stage V, as the hydration continues, the hydrates become more and more to form a barrier which blocks the way of solution flowing to make the unhydrated cement particles' reaction. Finally, movement through the

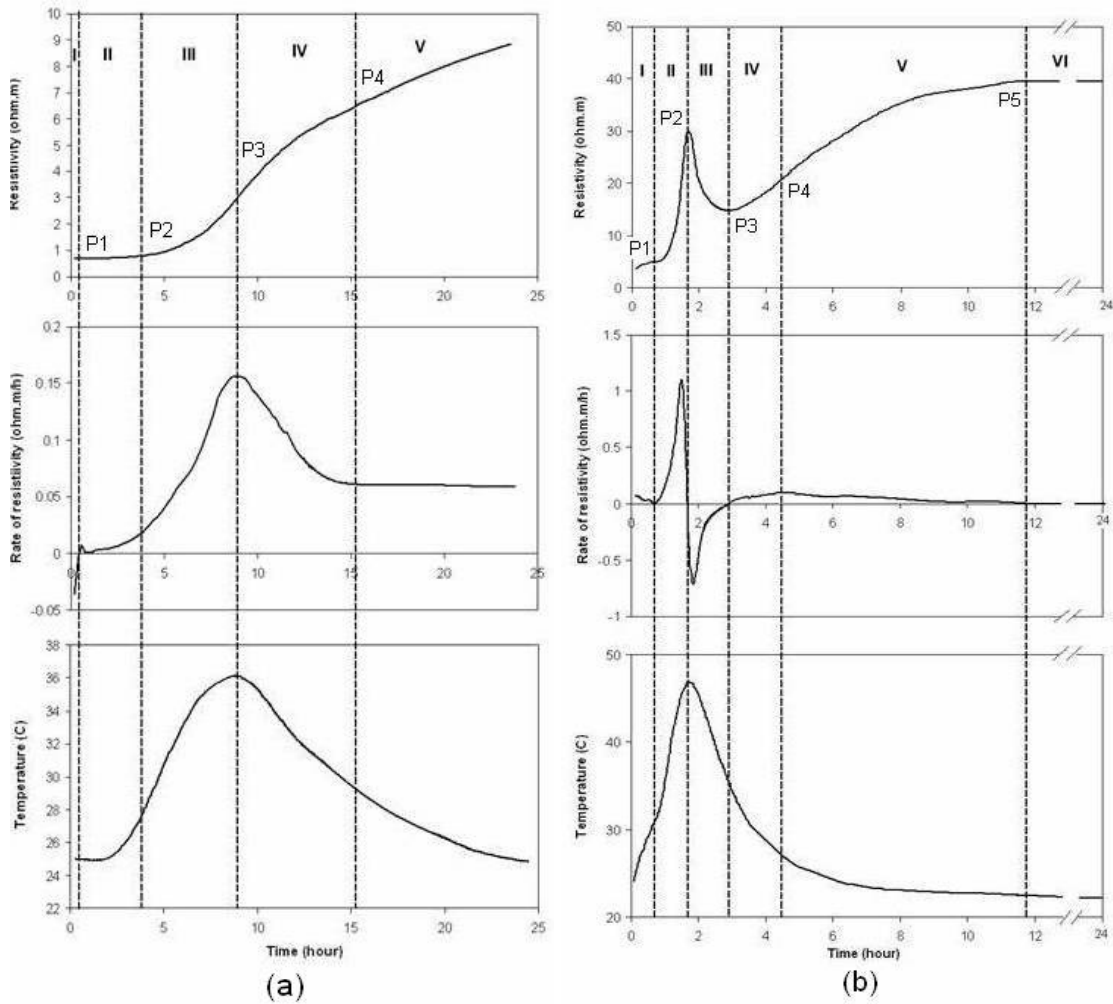


**Fig.5** Resistivity, rate of resistivity and temperature developments during the first 24 hours of hydration. (a) P03; (b) S055.

C-S-H layer determines the rate of reaction. The sample's resistivity development becomes ion diffusion controlled. Paste with higher W/C ratio needs a longer time to reach the certain hydration stage. Its hydration rate is slower than the lower W/C ratio paste, which correlated with the results of compressive strength test. From Table (2), we find a positive relationship between the electrical resistivity and the compressive strength, which can be written as:  $F_c=3.97\rho+0.64$  ( $R^2=0.9983$ ), in which the  $F_c$  represents the compressive strength (MPa) and  $\rho$  is the resistivity (ohm.m) at the same time of hydration.

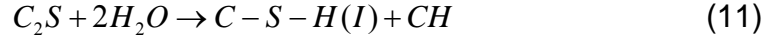
The electrical resistivity, the rate of resistivity and temperature developments of hydration of fresh CSA paste are shown in Fig. (5-b). All the samples with different W/C ratios have the similar behaviors too. Here we only show the typical resistivity, rate of resistivity and temperature curves of S055 during the first 24 hours of hydration. According to the behaviors of resistivity and temperature developments, the progress of the hydration reaction with time can be divided into six stages as shown in Fig. (5-b):

- I—dissolution and competition stage (0-0.9 hour);
- II—self-desiccation stage (0.9-1.7 hour);
- III—transformation from AFt to AFm stage (1.7-3 hour);
- IV—acceleration stage (3-4.5 hour);
- V—deceleration stage (4.5-12 hour); and
- VI—steady hardening stage (after 12 hour).

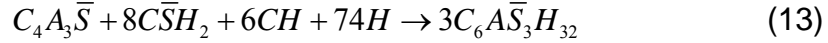
In Stage I, on the first mixing with water, ions in the clinker minerals are rapidly released from the surface of particles. The initial hydrolysis of CSA cement happens within 10 min after mixing, followed by a short competition period lasting only 10-20 min [10]. The competition period is caused by the need to achieve a certain concentration of ions in solution and the crystal nuclei from which the hydration products grow. The stage I of CSA cement's hydration process is similar to the dissolution and competition stages in the hydration of OPC paste, though quite a short time is needed due to the fast hydration. And the end of the competition period is corresponding to the setting time similarly with the OPC as shown in Table. (2).

In Stage II, reactions of the calcium sulfoaluminate and gypsum phases play a predominant role. Because as it is introduced before, the most distinctive feature of CSA cements is their content of  $C_4A_3\bar{S}$  and  $C\bar{S}H_2$ . Mechanisms of hydration in the  $C_4A_3\bar{S}$ - $C\bar{S}H_2$ - $H_2O$  system has been well-established [14]. When enough water and gypsum are available, ettringite ( $C_6A_3\bar{S}_3H_{32}$ , AFt) is the major product and small amount of monosulfate

( $C_4A\bar{S}H_{12}$ , AFm) can be produced. For the CSA cement we used in this study, ettringite is the dominant matrix former because about 38% gypsum was ground with the clinkers. Such water-rich hydration products need high W/C ratios to complete the hydration, or else self-desiccation occurs. The hydration of CSA cement leads to the rapid formation of ettringite, according to the equations [15]:



Combine the above equations



Equations are complex, but the reaction proceeds via the through-solution mechanism [16]. Calcium, sulfate and aluminate ions enter the solution, which rapidly becomes supersaturated with respect to ettringite. This reaction is an exothermic reaction which releases a lot of heat leading the rapid increase of temperature in the samples as shown in Fig. (5-b). Therefore, an initial skeleton of AFt (Fig.4), which contains a lot of crystallization water, forms rapidly and consumes nearly all the free water in the reaction because of the insufficient water added to make the hydration completely. The chemical water demand (CWD) for complete hydration of clinker used in this study is 0.54 [17]. Obviously, the W/C ratios (0.3-0.55) we used in the study are not enough for completing hydration though they can make workable pastes. As a consequence of their high CWD theoretically, CSA mixes readily undergo self-desiccation. Sufficient ettringite formed will consume all free water and thereafter ettringite continued to coexist with unhydrated clinker. The self-desiccation could cause a very high electrical resistivity of CSA pastes because less free water exists in the pore solution where the major ions' transportation occurs. The maximum resistivity is also corresponding to the maximum temperature.

In Stage III, there is a fast decrease of resistivity from the maximum. This decrease in the resistivity-time curve is actually due to two main effects [5]; these are:

1) The transformation of AFt to AFm.

AFt and AFm are unstable. They can transform to each other under the certain conditions [6]. At a higher temperature, when there is insufficient  $CaSO_4$  in the solution, the AFt phase will transform to AFm. Whereas, if there is enough  $CaSO_4$  in the solution, the AFm will transform to AFt under the normal temperature. At the end of the stage II, the CSA paste gains the internal self-desiccation, the reaction to produce AFt consumes a lot of  $CaSO_4$ , and the sample's temperature also reaches to the highest value. All of these satisfy the requirement of transformation from AFt to AFm:



Therefore, the transformation from AFt to AFm results in the release of  $2\text{Ca}^{2+}$  and  $2\text{SO}_4^{2-}$  gm ions per one mole of ettringite leading to an increase in the number of ions. However, this transformation phenomenon was quite difficult to be caught by the SEM test because (1) the AFm had lower crystallization and was not easy to be recognized from the SEM photos; and (2) the transformation phenomenon happened within several minutes so that it was hard to stop the hydration right at that time for preparing the SEM samples. Therefore, we can not observe any significant change of the microstructures (Fig.4) before and after the highest peak in the resistivity development.

2) The osmotic pressure development to split the pieces of the hydrates covering and the surface of cement grains, which is immediately accessible to water, leading to an increase in the ionic mobility.

As a consequence, we believe that the increase of ions' concentration and mobility leads to a sharp decrease in the resistivity. And this decrease of resistivity is also correlated to the decrease of temperature.

In Stage IV, with the decrease of temperature and the release of  $\text{CaSO}_4$  and water, more unhydrated cement particles are dissolved and the further hydration reaction happens. Because there are not enough water and gypsum, AFm will be the major hydration product:



Meanwhile, some of the AFm can transform to the AFt due to the lower temperature and sufficient water and  $\text{CaSO}_4$  in the certain local area. The rate of resistivity development will be accelerated, though the speed is much lower than the acceleration in Stage II.

In Stage V, with the hydration increase, more and more water and gypsum are consumed in the reaction. The reaction rate is decelerated as the deceleration stage in OPC cement.

In Stage VI, after about 12 hours, there is nearly no change in the resistivity curves showing the finish of major hydration of CSA cement, which was confirmed by the 7h and 24h's SEM pictures in Fig. (4). Different from the OPC cement, CSA paste has the negative relationship with the compressive strength (Table. 2). The mechanism of this situation needs to be clarified.

Table (2) summarizes the data for the electrical resistivity and other physical and mechanical properties (setting times, compressive strengths) of all the samples. For OPC cements, five stages of hydration corresponding to the stages of temperature can be defined to successfully describe the hydration process. The final setting time is accompanied by the end of the hydration Stage II (competition period). And a certain positive relation can be found between the compressive strength and the resistivity at the same hydration degree. Compared with OPC, the CSA

cements show the much fast hydration process from the electrical curves. Six hydration stages including the delta-shaped resistivity phenomenon can be defined. The final setting time is also correlated to the end of the competition period as the OPC cements. Whereas, the compressive strength and the resistivity show a negative relation.

**Table 2** Setting times and resistivity characteristic pints

Cement	W/C	Setting time (hour)		Transition point between hydration stages (hour)					Compressive strength at 24 hour (MPa)	Resistivity at 24 hour (ohm.m)
		IS	FS	P1	P2	P3	P4	P5		
OPC	0.3	2.92	4.3	0.47	3.85	8.97	15.2		37.13	9.27
	0.38	4.23	6.3	0.67	6.2	10	16.85		19.73	4.61
	0.44	5.17	7.8	0.83	8.02	10.78	20		11.06	2.62
	0.55	6.27	8.9	0.92	8.87	11.5	-		5.76	1.41
CSA	0.3	0.15	0.27	0.32	0.75	1.67	3.07	7.67	51.96	25.94
	0.38	0.23	0.42	0.57	1.02	1.93	3.8	7.87	46.84	35.14
	0.44	0.32	0.58	0.63	1.15	2.23	4.35	8.9	38.38	37.00
	0.55	0.43	0.92	0.85	1.68	2.97	4.53	11.9	27.50	39.45

## 5. Conclusions

The development in electrical resistivity reflects the physical and chemical changes in the cement paste and can be used to monitor the hydration processes. The relationship between electrical resistivity vs. time for Portland, as well as non-Portland cement pastes with the heat of hydration curves, suggests that the mechanism responsible for the resistivity of such systems can be related to their hydration mechanisms. The non-contacting resistivity measurement provides an accurate and effective way to determine and assess the characterization of the hydration properties of cement-based materials.

A good match has been found between electrical and thermal data. In the typical temperature and resistivity curves for the OPC and CSA cements, several hydration stages can be divided, which also match the hydration reactions very well. For CSA cement, its delta-resistivity phenomenon has been explored.

## References

---

- [1] G. Levita, A. Marchetti, G. Gallone, A. Princigallo, G.L. Guerrini, Electrical properties of fluidified Portland cement mixes in the early stage of hydration, *Cem Concr Res* 30 (6) (2000) 923-930
- [2] Z. Li, W. Li, Contactless, transformer-based measurement of the resistivity of materials, United States Patent 6639401 (2003)
- [3] Z. Li, X. Wei, W. Li, Preliminary interpretation of Portland cement hydration process using resistivity measurement, *ACI Mater J* 100 (3) (2003) 253-257
- [4] X. Wei, Z. Li, Study on hydration of Portland cement with fly ash using electrical measurement, *Mater and Struc* 38 (2005) 411-417
- [5] S.A. Abo El-Enein, M.F. Kotkata, G.B.Hana, M. Saad, M.M. Abd El Razek, Electrical conductivity of concrete containing silica fume, *Cem Concr Res* 25 (8) (1995) 1615-1620
- [6] Y. M. Wang, M. Z. Su, L. Zhang, Sulphoaluminate Cement, Beijing University of Technology Press, Beijing, 1999 (in Chinese)
- [7] F. P. Glasser, L. Zhang, High-performance cement matrices based on calcium sulfoaluminate-belite compositions, *Cem Concr Res* 31 (2001) 1881-1886
- [8] J. H. Sharp, C. D. Lawrence, R. Yang, Calcium sulfoaluminate cements—low-energy cements, special cements or what? *Adv Cem Res* 11 (1) (1999) 3-13
- [9] L. Zhang, F. P. Glasser, New concretes based on calcium sulfoaluminate cement, in: R. K. Dhir, D. Dyer, T. Telford (Eds.), *Proceedings of the International Conference on Modern Concrete Materials: Binders, Additions and Admixtures*, 1999, pp. 261– 274
- [10] L. Zhang, F. P. Glasser, Hydration of calcium sulfoaluminate cement at less than 24 h, *Adv Cem Res* 14 (4) (2002) 141-155
- [11] Z. Li, J. Zhang, Delta phenomenon in resistivity of calcium sulfoaluminate cement, *Cem Concr Res* (2006) Submitted
- [12] M. Perez-Pena, D.M. Roy, F.D. Tamás, Influence of chemical composition and inorganic admixtures on the electrical conductivity of hydrating cement pastes, *J Mater Res* 4 (1) (1989) 215-223
- [13] J.P. Skalny, J.F. Young, Mechanisms of Portland cement hydration, in: *Proceedings, 7<sup>th</sup> International Congress on the Chemistry of Cements*, Editions Septima, Paris, 1980, I, pp. II-1/3-II-1/45
- [14] F. Hanic, I. Kapralik, A. Gabrisova, Mechanism of hydration reactions in the system  $C_4A_3\bar{S}$ -CS-CaO-H<sub>2</sub>O referred to hydration of sulfoaluminate cements, *Cem Concr Res* 19 (1989) 671-682
- [15] J. Péra, J. Ambroise, New applications of calcium sulfoaluminate cement, *Cem Concr Res* 34 (2004) 671-676
- [16] H. F. W. Taylor, *Cement Chemistry*, Thomas Telford, London, ed. 2, 1997
- [17] F. P. Glasser, L. Zhang, Calculation of chemical water demand for hydration of calcium sulfoaluminate cement, Kuei Suan Jen Hsueh Pao/ *Journal of the Chinese Ceramic Society* 28 (4) (2000) 340-347 (in Chinese).